

Dynamics of Wetting and Phase Separation

P. Guenoun and D. Beysens

*Service de Physique du Solide et de Résonance Magnétique, Centre d'Etudes Nucléaires-Saclay,
91191 Gif-sur-Yvette CEDEX, France*

M. Robert

*Rice Quantum Institute and Department of Chemical Engineering, Rice University, P.O. Box 1892, Houston, Texas 77251
(Received 21 June 1989)*

The connection between the growth of a wetting layer and bulk phase separation is investigated in a liquid system undergoing spinodal decomposition. The wetting phase which grows at the walls of the container is found to be rippled and connected to the bulk, and layering of spatially anisotropic domains of the nonwetting phase is observed near the wall. Growth laws are determined and compared with a dimensional analysis of the Navier-Stokes equations.

PACS numbers: 64.60.Ht, 68.10.-m, 68.55.Gi

Most studies of the dynamics of wetting have been concerned with the case of the spreading of a droplet of a nonvolatile phase.¹ However, very little is known for the case of a wetting phase in equilibrium with its saturated vapor,^{2,3} which is very common in several technological processes and daily occurrences, e.g., in materials processing and in condensation on a substrate. It also applies to the separation of immiscible phases after stirring. In these cases bulk thermodynamic conditions (phase separation) are as important as wetting properties, and interactions of the surfaces with the bulk are essential. In fact, in contrast to what has been previously considered in theory,⁴ surface and bulk dynamics can strongly influence each other, as will be seen in the present study.

In this Letter we consider as a model system a binary fluid mixture near its consolute critical point. The choice of such a system is dictated by the fortunate situation with which dynamical properties can be determined experimentally during a long time period (we use a density-matched system to suppress gravity effects and study the growth at late times where optical observation is possible),⁵ as well as by the availability of scaling theories.⁶ Phase separation occurs here through spinodal decomposition, a common process in metallurgy and polymer science.^{6,7} In this process, the system is thermally quenched inside its spinodal region and evolves from the one-phase to the two-phase region according to complex and fascinating mechanisms. First, all fluctuations become unstable and grow with time depending on their size, favoring a typical wavelength L_m that gives rise to the well-known ring pattern in the scattered light.⁷ This process very soon leads to domains which are locally at the equilibrium concentrations and which coarsen in time, yielding an increasing L_m . If gravity effects are suppressed,⁵ the spatial structures keep growing with time, becoming visible under the optical microscope and ultimately reaching the dimensions of the sample cell it-

self. The fact that in the critical region the volume fraction of each phase is nearly 50% makes the growth very rapid due to capillary instabilities.⁸

In our basic experiment, a mixture of cyclohexane (C) and methanol (M) at critical concentration is thoroughly mixed in its one-phase region, at an initial temperature $T = T_i$ slightly above the critical temperature T_c . After mixing the system remains homogeneous. Typically $T_i - T_c = 1$ mK. The mixture is then quenched into its two-phase region at a final temperature $T_f < T_c$, where it phase separates through spinodal decomposition. The quench depth is defined as $T_c - T_f$. The questions of greatest interest are the following: How does the growth of a wetting film compare to that of the corresponding bulk phase, and how does the former modify the latter? For obvious practical reasons, the substrates considered here are the quartz container walls and the vapor phase. The final configuration of the system [Figs. 1(a)-1(e)] is that of a phase (M -rich or M_+) wetting the walls of the container and the vapor phase, and surrounding the nonwetting phase (C -rich or M_-).

The experimental setup has been described in Ref. 5, and we restrict ourselves here to those elements which are necessary to comprehend the present new results. The mixture of cyclohexane and methanol is weighted at its critical M -mass fraction $c_M = 0.294$, within 0.5%, under air at atmospheric pressure. In order to suppress gravity effects, which affect the growth of the fluid phases by external flows, we use a mixture of methanol (M) and partially deuterated cyclohexane (C). For a particular value of the deuteration ratio ($\approx 3\%$), comparative Earth-bound and space experiments⁵ have shown that gravity flows are negligible during most of the growth period. We have verified that no appreciable change in thickness of the wetting film with the height is observed during the observations.

The cell is a short cylinder of fused quartz of inner diameter $\phi = 20$ mm with flat windows on the ends having

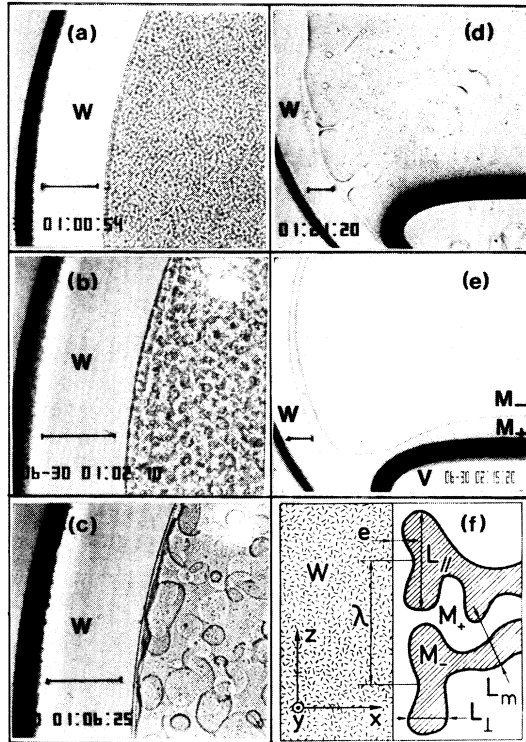


FIG. 1. (a)-(e) Different stages of phase separation for a quench of 2.5 mK. (a) 54 s; (b) 130 s; (c) 385 s; (d) 1280 s; (e) 4520 s. The horizontal bar represents 1 mm. *W* denotes the outer wall of the quartz cell. The axis of the cell is oriented horizontally, perpendicularly to the plane of the figure. Gravity is directed upwards. In (d) and (e) the thick black boundary corresponds to the meniscus of the liquid and the vapor (*V*), which is also wet by the *M*₊ phase. (f) Schematic illustration indicating the main growth parameters. The hatched region corresponds to the *M*₋ phase.

an inner separation of $l_0 = 2.00$ mm. Sealing is ensured by a Teflon screw tap. The cell is immersed in a water-bath thermostat with long-term regulation of ± 0.3 mK. Temperature is measured with a sensor located close to the cell. Thermalization of the sample is directly measured by light transmission measurements above T_c . The latter shows that temperature quenches are performed with an unavoidable time constant due mainly to the time, of order 15 s, that heat takes to diffuse through the cell walls and the mixture, while the bath equilibrates in roughly 10 s.

Direct visual observations have been performed. The image is formed by light scattered at small angles, and thus by the interfaces perpendicular to the plane of the image.⁵ An image of the sample with different magnification ratios, corresponding to a field of view ranging from 300 μ m to 20 mm, is formed on the sensitive array of a charge-coupled-device camera (512 \times 512 pixels). The images are stored in a video recorder, and are analyzed either manually on a planar television monitor or with a computer (16 bits) after digitization over 6 bits.

The useful numerical constants of the system are^{5,9} the correlation length of the bulk concentration fluctuations in the two-phase region, $\xi_- = 1.6\epsilon^{-0.63}$ Å, and their associated typical lifetime $t_- = 6\pi\eta(\xi_-)^3/k_B T = 1.23\epsilon^{-1.89} \times 10^{-11}$ s. Here $\eta \approx 7 \times 10^{-3}$ (cgs units) is the shear viscosity, k_B is Boltzmann's constant, T (K) is the temperature, and $\epsilon = 1 - T/T_c$, with $T_c = 318$ K the critical temperature.

Typical growth patterns are shown in Figs. 1 and 2. [The characteristic lengths are defined in Fig. 1(f).] We observe the following: (i) The domains in the bulk form a bicontinuous pattern with typical wavelength L_m [Fig. 1(a)]. This bulk pattern has already been studied in detail in this system; growth is due to capillary flows.⁸ (ii) The wetting layer, of average thickness e , is rippled with wavelength λ . Strictly speaking, this wetting phase does not form a film since it is connected to the bulk, as is seen from Figs. 1(d) and 2. (iii) A remarkable layering of spatially anisotropic domains of the nonwetting phase is observed between the wetting layer and the bulk (Fig. 2). The typical lengths of these domains, in the directions parallel and perpendicular to the substrate, are denoted L_{\parallel} and L_{\perp} , respectively [Fig. 1(f)].

It appears, when considering Figs. 1(a)-1(c), which correspond to different growth times, and when taking into account the finiteness of the optical resolution,⁵ that a mere change of scale makes the bulk patterns at different growth stages self-similar. This observation can be made more precise, by considering the typical length scales in the problem, which are set by the bulk correlation length ξ_- and the cell dimensions l_0 and ϕ . The only time scale is the typical time t_- associated with concentration fluctuations of size ξ_- . Scaling by ξ_- applies as long as L_m is smaller than both l_0 and ϕ , and, when expressed in scaled units, the behavior of $L_m^* = L_m/\xi_-$ with respect to the scaled time $t^* = t/t_-$ is universal in this regime. Therefore all experimental data obtained at different times and at different quench depths lie on a single, universal curve.^{5,10} There is no reason to question scaling for the above parameters L_a ($L_a = \{e, \lambda, L_{\parallel}, L_{\perp}, L_m\}$), since the only length scale for them is also ξ_- . All the L_a should therefore lie on a universal curve pro-

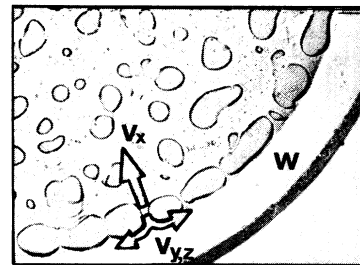


FIG. 2. Photograph taken at a quench depth of 5 mK at $t = 11$ s showing how the domains of the nonwetting phase coalesce and induce ripples of the wetting layer. The flow velocities ($V_{x,y,z}$) are defined in the text.

vided they are expressed as functions of t^* in the scaled units $L_a^* = L_a/\xi$ – or equivalently $K_a^* = 2\pi\xi_-/L_a$. Scaling, however, should break down when L_a is larger than l_0 or ϕ . As can be seen from Fig. 1(d), this new regime is accompanied by the disconnection of the wetting film from the corresponding phase still remaining in the M – phase. A final state is reached where the wetting phase surrounds the nonwetting phase, in which many tiny isolated domains of the former are still present [Figs. 1(d) and 1(e)]. A rough estimate of the total volume of the wetting layer shows it to consist of 25% of the wetting phase, with isolated droplets making up the remaining 75%. Note that this dispersed phase has no chance of growing during the time of an experiment in the absence of external-field effects: The domains are too large to move appreciably by Brownian motion or to exhibit a noticeable concentration deviation with respect to equilibrium which would lead to an evaporation-condensation growth mechanism.¹¹

We next describe our quantitative results. First, L_{\perp} is seen to behave like L_m , and L_{\parallel} like λ . The reason for this behavior can be found in the growth process itself (Fig. 2). Growth of domains of the nonwetting phase is not much affected in the direction perpendicular to the substrate, leading to $L_{\perp} \propto L_m$. This simply reflects the fact that coalescence events occurring perpendicularly to the substrate are not modified by the presence of the substrate. The fact that the M – phase does not wet the substrate leads to a layering of M – domains parallel to the substrate. This layering favors coalescence and flow in a plane parallel to the substrate, making the nonwetting domains spatially anisotropic and accounting for $L_{\parallel} > L_{\perp}$. The wetting film is in turn interconnected to its corresponding bulk phase across the plane formed by the domains of the nonwetting phase. Consequently, the wavelength λ of the ripples, a reminiscence of the interconnection, is proportional to L_{\parallel} , as is seen in Fig. 2. The growth of L_{\parallel} occurs mainly by steps due to coalescence events in a plane parallel to the substrate. The growth of λ is an average of such events with much better statistics, and in the following we will therefore report only the λ measurements.

Figure 3 shows the behavior with respect to t^* of the reduced growth parameters (K_a^*). Different quench depths have been investigated: 1.5, 2.5, 5, and 10 mK. Each data point corresponds typically to an average over five measurements. The standard deviation is difficult to define because of the poor line statistics. We estimate it to be 10%. The behavior of the growth parameters is seen to support the scaling ideas described above. It is interesting to note that the scaled layer thickness e^* remains 10 times smaller than all other lengths, the latter ultimately becoming of the same order.

The time evolution of the parameters K_a^* is found to be well described by the power laws $K_m^* \sim K_{\perp}^* \sim t^{*-1}$, $K_{\lambda}^* \sim K_{\parallel}^* \sim t^{*-a}$ with $a = 0.64 \pm 0.15$, and $K_e^* \sim t^{*-b}$

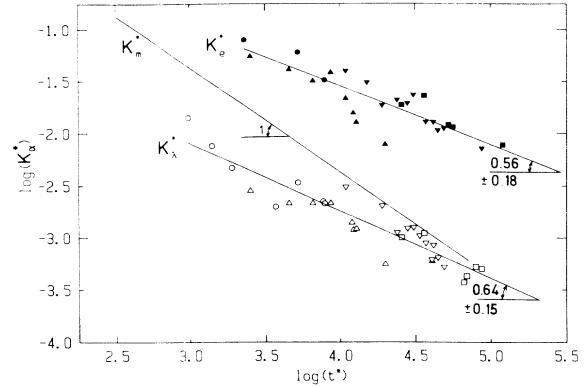


FIG. 3. Behavior in scaled units of the growth parameters $K_a^* = 2\pi\xi_-/L_a$, with $L_a = (L_m, e, \lambda)$; t^* is a reduced time. Open symbols (\circ , \triangle , ∇ , \square) refer to the quench depths $T_c - T_f = 1.5, 2.5, 5$, and 10 mK, respectively, for K_{λ}^* . Solid symbols (\bullet , \blacktriangle , \blacktriangledown , \blacksquare) refer to the same quench depths for K_e^* . The line of slope unity represents the behavior of $K_m^* \propto K_{\perp}^*$ (for clarity, data points are not reported; they are in agreement with those from Refs. 5 and 10).

with $b = 0.56 \pm 0.18$. The values of a and b have been obtained by a least-squares fit, and the uncertainties correspond to 3 standard deviations. The linear time dependence of K_m^* is well known¹⁰ and reflects a very rapid growth by capillary flow in the 3D interconnected domain pattern. This capillary flow is attributed to an instability, a dimensional argument⁸ leading to $(K_m^*)^{-1} \sim (\sigma/\eta)t^*$, where σ is the interfacial tension. The exponents associated with the growth of the layering domains and with that of the wetting film are more difficult to interpret. From Figs. 1 and 2 it seems clear nevertheless that growth also proceeds in this case through a hydrodynamic process, but with geometric limitations due to the presence of the substrate. However, the wetting film should not develop by itself the same capillary instability that drives growth in the bulk;¹² its growth can only be attributed to flow from the bulk.

The growth process can be analyzed in detail as follows (Fig. 2). The volume increase of the wetting layer per unit area is assumed to be proportional to the incoming flux perpendicular to the substrate $\dot{e} = de/dt \propto N_L \times L^2 V_x$, where N_L is the number of interconnections per unit area, L^2 is the average area of these interconnections, and V_x is the flow velocity in the direction normal to the substrate. Since $N_L \sim \lambda^{-2}$ [Fig. 1(f)], and because L should scale as λ , one finds $\dot{e} \propto \lambda^{-2} \lambda^2 V_x = V_x$. That is to say, the growth velocity of the film is proportional to the flow velocity in the direction normal to the substrate. Assuming the flow to be due to bulk capillary instability, the Navier-Stokes equations read, in direction x , with p the capillary pressure,

$$(\nabla p)_x = \sigma(L_m e)^{-1} = \eta \Delta V_x \propto \eta \left[\frac{\dot{e}}{e^2} + \frac{2\dot{e}}{\lambda^2} \right]. \quad (1)$$

As $L_m \sim t$, Eq. (1) leads to a differential equation with solution $\lambda \sim e$ and $\dot{e}/e \sim t^{-1}$, implying that both λ and e obey the same power law with a single exponent $a=b$. In the directions y, z , the Navier-Stokes equations give

$$\begin{aligned} (\nabla p)_{y,z} &= \sigma(L_m \lambda)^{-1} \\ &= \eta \Delta V_{y,z} \propto \eta \left(\frac{V_{y,z}}{e^2} + \frac{2V_{y,z}}{\lambda^2} \right), \end{aligned} \quad (2)$$

which, after straightforward algebra, leads to $V_{y,z} \sim \dot{\lambda}$ which is similar to the result $V_x \sim \dot{e}$. The prediction $a=b$ is consistent with the present experimental findings. Unfortunately, in contrast to the bulk case, this approach does not enable us to determine the value of the exponents.

We thank Constance Valentin for help with the measurements. This work has been partially supported by the Centre National d'Etudes Spatiales and the Indo-French Center for the Promotion of Advanced Research, as well as by the U.S. National Science Foundation, the Welch Foundation, and the Petroleum Research Fund administered by the American Chemical Society.

¹P. G. de Gennes, in *Liquids at Interfaces*, edited by J. F.

Joanny and J. Zinn-Justin (Elsevier, Amsterdam, 1990); A. M. Cazabat, *ibid.*

²S. Dietrich, in *Phase Transitions and Critical Phenomena*, edited by C. Domb and J. L. Lebowitz (Academic, New York, 1988), Vol. XII.

³D. J. Durian and C. Franck, *Phys. Rev. A* **40**, 5220 (1989).

⁴R. Lipowsky and D. A. Huse, *Phys. Rev. Lett.* **57**, 353 (1986).

⁵P. Guenoun, R. Gastaud, F. Perrot, and D. Beysens, *Phys. Rev. A* **36**, 4876 (1987); D. Beysens, P. Guenoun, and F. Perrot, *Phys. Rev. A* **38**, 4173 (1988), and references therein.

⁶*Dynamics of Ordering Processes*, edited by S. Komura and H. Furukawa (Plenum, New York, 1988).

⁷J. W. Cahn, in *Critical Phenomena in Alloys, Magnets, and Superconductors*, edited by R. E. Milla, A. Ascher, and R. I. Jaffe (McGraw-Hill, New York, 1971).

⁸E. D. Siggia, *Phys. Rev. A* **20**, 595 (1979).

⁹C. M. Sorensen, R. C. Mockler, and W. J. O'Sullivan, *Phys. Rev. A* **16**, 365 (1977).

¹⁰W. I. Goldburg, in *Scattering Techniques Applied to Supramolecular and Nonequilibrium Systems*, edited by S. H. Chen, B. Chu, and R. Nessel (Plenum, New York, 1981); N. C. Wong and C. M. Knobler, *J. Chem. Phys.* **69**, 725 (1978).

¹¹M. Marder, *Phys. Rev. A* **36**, 858 (1987), and references therein.

¹²V. G. Levich, *Physicochemical Hydrodynamics* (Prentice-Hall, Englewood Cliffs, NJ, 1962).

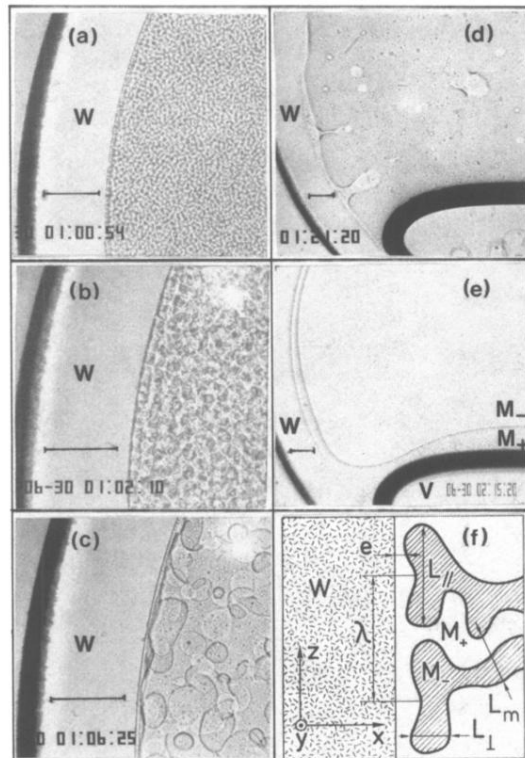


FIG. 1. (a)–(e) Different stages of phase separation for a quench of 2.5 mK. (a) 54 s; (b) 130 s; (c) 385 s; (d) 1280 s; (e) 4520 s. The horizontal bar represents 1 mm. W denotes the outer wall of the quartz cell. The axis of the cell is oriented horizontally, perpendicularly to the plane of the figure. Gravity is directed upwards. In (d) and (e) the thick black boundary corresponds to the meniscus between the liquid and the vapor (V), which is also wet by the M_+ phase. (f) Schematic illustration indicating the main growth parameters. The hatched region corresponds to the M_- phase.

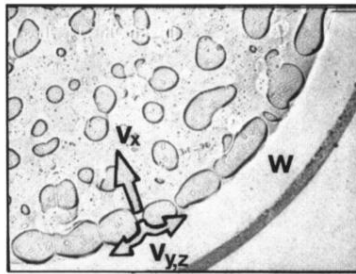


FIG. 2. Photograph taken at a quench depth of 5 mK at $t = 11$ s showing how the domains of the nonwetting phase coalesce and induce ripples of the wetting layer. The flow velocities ($V_{x,y,z}$) are defined in the text.